Nanostructures

DOI: 10.1002/anie.201207469

Integrated and Segregated Au/γ-Fe_2O_3 Binary Nanoparticle Assemblies**

*Meital Boterashvili, Michal Lahav, Tanya Shirman, Dalia Freeman, and Milko E. van der Boom**

Multicomponent materials might display synergistic effects and possess functions not attainable with single-component systems.[1,2] Control over the composition and structure of such materials is not trivial because many factors are involved (e.g., weak intermolecular forces, covalent interactions, solvent effects).[1–4] Moreover, control of phase segregation is essential and of high importance in material science[5–13] and biomolecular systems.[6,14] For instance, segregation of polymer blends is directly related to efficient charge-carrier generation and transport in solar cells.[8–10] Langer et al. used this phenomenon to develop shape-memory materials for biomedical applications.[14] Phase-separation is also used in the formation of Janus nanoparticles.[15] Achieving structural control of binary nanoparticle (NP) assemblies offers a promising route towards new materials as recently shown by Murray and others.[16–18] Such systems consist of integrated assemblies (IAs),[16–21] whereas segregated assemblies (SAs) are less common and mainly originate from size-dependent phase-separation.[17,22,23]

Herein we show the controlled and selective formation of both integrated assemblies and segregated assemblies with Au and γ-Fe_2O_3 NPs (Scheme 1). These systems were designed to comprise both the optical properties of AuNPs and the magnetic properties of γ-Fe_2O_3 NPs.[20,21,24,25] Bifunctional ligand **1** exhibits orthogonal reactivity towards these NPs.[26] We found that under certain reaction conditions the *N*-oxide moiety can bind both NPs, whereas the pyridine group exclusively binds to the AuNPs (Scheme S2, Table S1 in the Supporting Information).[27–29] Using the orthogonal reactivity of this cross-linker (**1**) with NPs, we succeeded to generate integrated assemblies. Replacing the vinylpyridine moiety of **1** with a styryl group (ligand **2**) resulted in the one-pot formation of the segregated assemblies. In addition, we also demonstrate the stepwise formation of segregated assemblies by using AuNP assemblies as nucleation surfaces for domains composed of γ-Fe_2O_3 NPs. These new assemblies were characterized by combining UV/Vis spectroscopy, transmission electron microscopy (TEM), energy dispersive X-ray spectroscopy (EDS), and cryogenic- (cryo-) TEM.

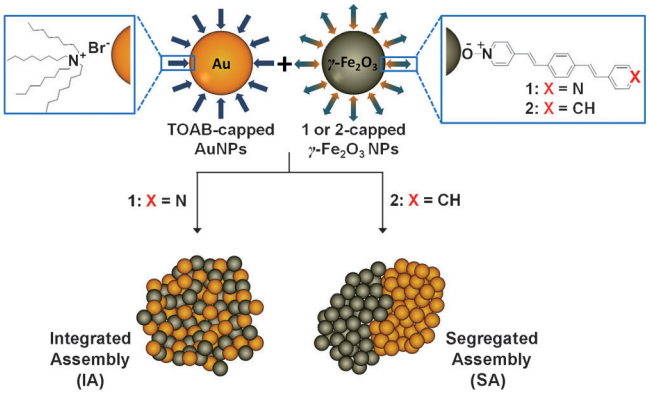

Scheme 1. Schematic representation of an integrated assembly (left) and a segregated assembly (right) formed upon treating **1**- or **2**-capped γ-Fe_2O_3 NPs with TOAB-capped AuNPs. The presence of free ligand causes also some self-aggregation of AuNPs.

Ligands **1** and **2** were dissolved in CH_2Cl_2 and added to THF-diluted solutions of oleic acid (OA)-capped γ-Fe_2O_3 NPs in toluene (Scheme S2, Table S1). Then, ligand (**1** or **2**)-capped γ-Fe_2O_3 NPs were treated with tetraoctylammonium bromide (TOAB)-capped AuNPs in solution to form integrated assemblies or segregated assemblies, respectively (Scheme 1). The addition of a **1**-capped γ-Fe_2O_3 NP light-yellow solution to TOAB-capped AuNPs resulted in an immediate color change. The pink AuNP solution turned purple (Figure 1 A, inset). Indeed, UV/Vis spectroscopy showed significant changes in the surface-plasmon resonance (SPR) band, demonstrating a 33 nm red shift, signal broadening and an increase in the intensity (Figure 1 A). This behavior is indicative of the formation of AuNP-containing aggregates.[28–30]

TEM analysis unambiguously showed the formation of integrated binary Au/γ-Fe_2O_3 NP assemblies, whereas the NPs retain their original size (AuNP: 5.0 ± 1.0 nm; γ-Fe_2O_3 NPs: 4.5 ± 0.5 nm) and shape (Figure 2 A and Figure S3 A). The Au and γ-Fe_2O_3 NPs are readily distinguishable as a result of their atomic number differences (Au: 79; Fe: 26), resulting in a brighter image for the γ-Fe_2O_3 NPs and a darker image for the AuNPs.[19] EDS measurements reveal the presence of both Au and Fe (Figure 3, compare the background spectrum (a) with spectrum (b)). In addition, cryo-TEM measurements

[*] M. Boterashvili, Dr. M. Lahav, Dr. T. Shirman, Dr. D. Freeman, Prof. M. E. van der Boom
Department of Organic Chemistry, Weizmann Institute of Science
Rehovot-76100 (Israel)
E-mail: milko.vanderboom@weizmann.ac.il
Homepage: http://www.weizmann.ac.il/oc/vanderboom/

[**] This research was supported by the Helen and Martin Kimmel Center for Molecular Design and the Minerva Foundation. Cryo-TEM measurements were performed by Dr. E. Kesselman (Technion). We thank Dr. R. Popovich-Biro (WIS) for the EDS measurements and Dr. R. Klajn (WIS) for the OA-capped γ-Fe_2O_3 NPs. M.E.v.d.B. is the incumbent of the Bruce A. Pearlman Professorial Chair in Synthetic Organic Chemistry.

Supporting information for this article is available on the WWW under http://dx.doi.org/10.1002/anie.201207469.

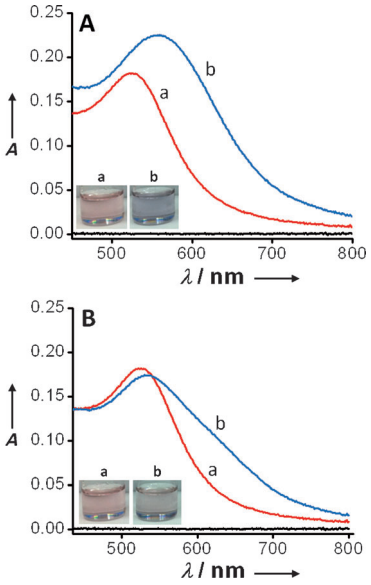

Figure 1. UV/Vis spectra for A) a) TOAB-capped AuNPs and b) the integrated assemblies and B) a) TOAB-capped AuNPs and b) segregated assemblies. The baseline is shown in black. Insets: photographs of the corresponding solutions.

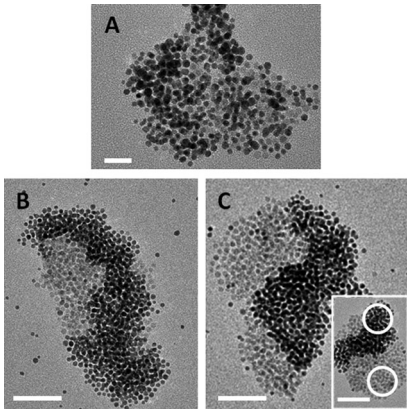

Figure 2. Representative TEM images of A) integrated assemblies and (B, C) segregated assemblies. C) Inset: The white circles indicate the areas analyzed by EDS (Figure 3); Top circle: the AuNPs domain, and bottom circle: the γ-Fe_2O_3 NPs domain, corresponding to EDS spectra (c) and (d), respectively (in Figure 3). Scale bar in (A) = 20 nm, in (B,C) and (C) inset = 50 nm.

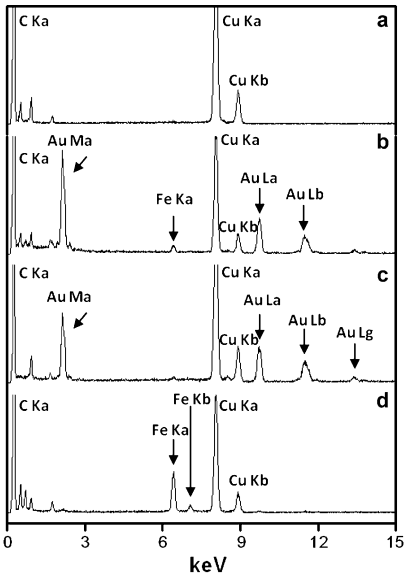

Figure 3. EDS spectra of a) TEM grid background, b) integrated assembly, c) the AuNP-domain in a segregated assembly and d) the γ-Fe_2O_3 NP-domain in a segregated assembly. The scale of the *y* axis is identical for all spectra. The arrows indicate the elemental peaks of Au and Fe. TEM images of these aggregates and the analyzed domains are shown in Figure S4 (integrated assembly) and in the inset of Figure 2C (segregated assembly).

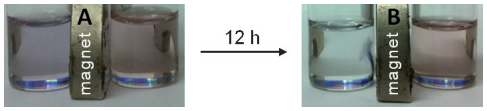

Figure 4. Photographs taken A) at $t = 0$ and B) after 12 h of exposing solutions containing integrated assemblies (left vial) and segregated assemblies (right vial) to a permanent magnet.

show the formation of aggregates in solution (Figure S5), ruling out drying effects. A solution containing these integrated assemblies was exposed to a permanent magnet.[20,21] A dark precipitate started to form after about 2 h in proximity with the magnet resulting, after approximately 12 h, in a colorless solution (Figure 4). As expected, UV/Vis spectroscopy of this solution showed a significant intensity decrease of the SPR band (Figure S6A). Almost no NPs or assemblies thereof were observed in a TEM analysis of the resulting solution. No precipitation or color change was observed in the absence of a magnetic field. The formation of the integrated assemblies can be attributed to coordination of the *N*-oxide group of ligand **1** to γ-Fe_2O_3 NPs and the pyridine moiety of this ligand to the AuNPs.[28,29]

The addition of a light yellow solution of **2**-capped γ-Fe_2O_3 NPs to a pink solution of TOAB-capped AuNPs resulted in only a slight color change of the AuNPs solution (Figure 1B, inset), a small 5 nm red shift and broadening of the SPR band (Figure 1B). These minor optical changes indicate the formation of smaller aggregates than observed for integrated assemblies (over 500 nm; Figure S3A). TEM measurements confirmed the formation of these aggregates (50–250 nm) composed of segregated Au and γ-Fe_2O_3 NP domains (Figure 2B and C, Figure S3B and C). High-resolution TEM images of the domain interfaces of these segregated assemblies do not show fusion or evident lattice matching,[31] while exhibiting clear domain boundaries (Figure S7). EDS analysis confirmed that each domain consists almost exclusively of Au or γ-Fe_2O_3 NPs (Au or Fe atomic % > 95; Figure 3, spectra (c) and (d), respectively). Cryo-TEM measurements confirmed the formation of the segregated assemblies in solution (Figure 5A and B). Applying a permanent magnet to the solutions did not result in a notable color change (Figure 4). Nevertheless, UV/Vis spectroscopy of the remaining solution showed a decrease in intensity and a 5 nm

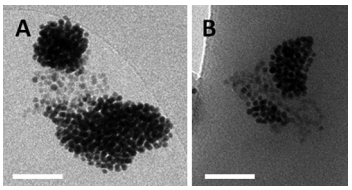

Figure 5. A) and B) Representative cryo-TEM images of segregated assemblies formed upon treating **2**-capped γ-Fe_2O_3 NPs with TOAB-capped AuNPs. Scale bar = 50 nm.

blue shift of the SPR band (Figure S6B). In agreement with the optical data, the TEM analysis showed only some separated AuNPs (Figure S8). No segregated assemblies were observed.

Mechanistically, the formation of the segregated assemblies might involve the initial formation of AuNP/**2** aggregates acting as a nucleation site for the γ-Fe_2O_3 NPs (Scheme 2).[32,33] This hypothesis is based on the TEM analysis of the reaction between **2**-capped γ-Fe_2O_3 NPs (containing free ligand **2**) and TOAB-capped AuNPs. Some aggregates of AuNP/**2** were observed in addition to the segregated assemblies (Figure S9). This process might be driven by π–π stacking.[34] These aggregates can also be generated directly by treating ligand **2** with TOAB-capped AuNPs as shown by UV/Vis spectroscopy (Figure S11B) and TEM measurements (Figure S12B). Remarkably, the addition of **2**-capped γ-Fe_2O_3 NPs to AuNP/**2** aggregates results in the stepwise formation of segregated assemblies (Figure S14C and D). The **2**-capped γ-Fe_2O_3 NPs do not aggregate in the absence of AuNPs (Table S1) and no free-standing assemblies thereof were observed in the presence of AuNP/**2** aggregates. This result implies that the modified gold surface induces the domain formation.

Stepwise domain formation might be a general approach towards the formation of segregated assemblies. The addition of a solution of ligand **1** to TOAB-capped AuNPs, resulted in the formation of AuNP/**1** aggregates as judged by UV/Vis spectroscopy and TEM measurements (Figure S11A and S12A). The addition of **1**-capped γ-Fe_2O_3 NPs to these AuNP/**1** aggregates resulted also in the formation of segregated assemblies (Figure S14A and B). The AuNP domains of these segregated assemblies reflect the pre-formed AuNP/**1** or **2** aggregates, which surface induced the aggregation of the **1**- or **2**-capped γ-Fe_2O_3 NPs (Scheme 2).

In conclusion, we have demonstrated that the structural arrangement of Au/γ-Fe_2O_3 binary NP assemblies can be controlled as a function of the capping layer, resulting in integrated and segregated assemblies. The use of orthogonal coordination chemistry resulted in the formation of integrated assemblies, whereas the use of NP-ligand coordination or π–π stacking resulted in well-separated domains (segregated assemblies). This formation of segregated assemblies reflects the importance and the use of hierarchical forces for phase-separation with NPs.[29,35] Our data show that AuNP/**1**- and AuNP/**2**-based assemblies promote the aggregation of the corresponding **1**- and **2**-capped γ-Fe_2O_3 NPs. Interestingly, the initial state of the AuNPs (i.e., non-aggregated or aggregated) directs the assembly mode of the NPs and can be used to form the segregated assemblies in a consecutive manner.

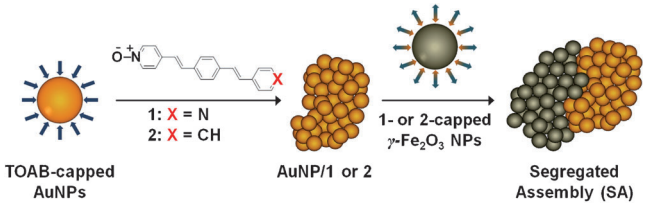

Scheme 2. Schematic representation of segregated assemblies formed upon treating AuNP/**1** or AuNP/**2** assemblies with **1**- or **2**-capped γ-Fe_2O_3 NPs, respectively.

Received: September 15, 2012
Published online: November 7, 2012

Keywords: aggregation · gold · iron oxide · nanoparticle assembly · nanostructures

[1] H. Zheng, Y. Li, H. Liu, X. Yin, Y. Li, *Chem. Soc. Rev.* **2011**, *40*, 4506 – 4524.
[2] S. J. Hurst, E. K. Payne, L. Qin, C. A. Mirkin, *Angew. Chem.* **2006**, *118*, 2738 – 2759; *Angew. Chem. Int. Ed.* **2006**, *45*, 2672 – 2692.
[3] A. J. Mieszawska, R. Jalilian, G. U. Sumanasekera, F. P. Zamborini, *Small* **2007**, *3*, 722 – 756.
[4] A. C. Balazs, T. Emrick, T. P. Russell, *Science* **2006**, *314*, 1107 – 1110.
[5] M. Boltau, S. Walheim, J. Mlynek, G. Krausch, U. Steiner, *Nature* **1998**, *391*, 877 – 879.
[6] T. Kato, *Science* **2002**, *295*, 2414 – 2418.
[7] S. Coe, W.-K. Woo, M. Bawendi, V. Bulovic, *Nature* **2002**, *420*, 800 – 803.
[8] J. K. J. van Duren, X. Yang, J. Loos, C. W. T. Bulle-Lieuwma, A. B. Sieval, J. C. Hummelen, R. A. J. Janssen, *Adv. Funct. Mater.* **2004**, *14*, 425 – 434.
[9] W. U. Huynh, J. J. Dittmer, W. C. Libby, G. L. Whiting, A. P. Alivisatos, *Adv. Funct. Mater.* **2003**, *13*, 73 – 79.
[10] M. Helgesen, R. Sondergaard, F. C. Krebs, *J. Mater. Chem.* **2010**, *20*, 36 – 60.
[11] B. N. Wanjala, J. Luo, R. Loukrakpam, B. Fang, D. Mott, P. N. Njoki, M. Engelhard, H. R. Naslund, J. K. Wu, L. Wang, O. Malis, C.-J. Zhong, *Chem. Mater.* **2010**, *22*, 4282 – 4294.
[12] B. N. Wanjala, J. Luo, B. Fang, D. Mott, C.-J. Zhong, *J. Mater. Chem.* **2011**, *21*, 4012 – 4020.
[13] S. J. Stranick, A. N. Parikh, Y.-T. Tao, D. L. Allara, P. S. Weiss, *J. Phys. Chem.* **1994**, *98*, 7636 – 7646.
[14] A. Lendlein, R. Langer, *Science* **2002**, *296*, 1673 – 1676.
[15] M. Lattuada, T. A. Hatton, *Nano Today* **2011**, *6*, 286 – 308.
[16] J. J. Urban, D. V. Talapin, E. V. Shevchenko, C. R. Kagan, C. B. Murray, *Nat. Mater.* **2007**, *6*, 115 – 121.
[17] H. Zeng, J. Li, J. P. Liu, Z. L. Wang, S. Sun, *Nature* **2002**, *420*, 395 – 398.
[18] E. V. Shevchenko, M. Ringler, A. Schwemer, D. V. Talapin, T. A. Klar, A. L. Rogach, J. Feldmann, A. P. Alivisatos, *J. Am. Chem. Soc.* **2008**, *130*, 3274 – 3275.
[19] D. V. Talapin, E. V. Shevchenko, M. I. Bodnarchuk, X. Ye, J. Chen, C. B. Murray, *Nature* **2009**, *461*, 964 – 967.
[20] X. Xu, N. L. Rosi, Y. Wang, F. Huo, C. A. Mirkin, *J. Am. Chem. Soc.* **2006**, *128*, 9286 – 9287.
[21] Z. Chen, J. Li, X. Zhang, Z. Wu, H. Zhang, H. Sun, B. Yang, *Phys. Chem. Chem. Phys.* **2012**, *14*, 6119 – 6125.

[22] C. J. Kiely, J. Fink, M. Brust, D. Bethell, D. J. Schiffrin, *Nature* **1998**, *396*, 444 – 446.
[23] J. Cheon, J.-I. Park, J.-s. Choi, Y.-w. Jun, S. Kim, M. G. Kim, Y.-M. Kim, Y. J. Kim, *Proc. Natl. Acad. Sci. USA* **2006**, *103*, 3023 – 3027.
[24] M.-C. Daniel, D. Astruc, *Chem. Rev.* **2004**, *104*, 293 – 346.
[25] Y.-w. Jun, J.-s. Choi, J. Cheon, *Chem. Commun.* **2007**, 1203 – 1214.
[26] B. M. Leonard, M. E. Anderson, K. D. Oyler, T.-H. Phan, R. E. Schaak, *ACS Nano* **2009**, *3*, 940 – 948.
[27] T. Shirman, T. Arad, M. E. van der Boom, *Angew. Chem.* **2010**, *122*, 938 – 941; *Angew. Chem. Int. Ed.* **2010**, *49*, 926 – 929.
[28] M. Orbach, M. Lahav, P. Milko, S. G. Wolf, M. E. van der Boom, *Angew. Chem.* **2012**, *124*, 7254 – 7257; *Angew. Chem. Int. Ed.* **2012**, *51*, 7142 – 7145.
[29] R. Kaminker, M. Lahav, L. Motiei, M. Vartanian, R. Popovitz-Biro, M. A. Iron, M. E. van der Boom, *Angew. Chem.* **2010**, *122*, 1240 – 1243; *Angew. Chem. Int. Ed.* **2010**, *49*, 1218 – 1221.
[30] L. Beverina, *ChemPhysChem* **2010**, *11*, 2075 – 2077.
[31] T. Sehayek, M. Lahav, R. Popovitz-Biro, A. Vaskevich, I. Rubinstein, *Chem. Mater.* **2005**, *17*, 3743 – 3748.
[32] J. Chen, Y. Xiong, Y. Yin, Y. Xia, *Small* **2006**, *2*, 1340 – 1343.
[33] A. Dey, P. H. H. Bomans, F. A. Müller, J. Will, P. M. Frederik, G. de With, N. A. J. M. Sommerdijk, *Nat. Mater.* **2010**, *9*, 1010 – 1014.
[34] Z. Shen, M. Yamada, M. Miyake, *J. Am. Chem. Soc.* **2007**, *129*, 14271 – 14280.
[35] J.-M. Lehn, *Angew. Chem.* **1988**, *100*, 91 – 116; *Angew. Chem. Int. Ed. Engl.* **1988**, *27*, 89 – 112.

